

Electrochemical Reduction of N₂O with a Molecular Copper Catalyst

Jorge L. Martinez, Joseph E. Schneider, Sophie W. Anferov, and John S. Anderson*

Department of Chemistry, University of Chicago, Chicago, Illinois 60637, United States.

KEYWORDS: N₂O reduction, N₂O reductase, homogenous catalysis, electrocatalysis, redox-active ligand, denitrification

ABSTRACT: Deoxygenation of nitrous oxide (N₂O) has significant environmental implications as it is not only a potent greenhouse gas but is also the main substance responsible for the depletion of ozone in the stratosphere. This has spurred significant interest in molecular complexes that mediate N₂O deoxygenation. Natural N₂O reduction occurs via a Cu cofactor but there is a notable dearth of synthetic molecular Cu catalysts for this process. In this work, we report a selective molecular Cu catalyst for the electrochemical reduction of N₂O to N₂ using H₂O as a proton source. Cyclic voltammograms show that increasing H₂O concentration facilitates deoxygenation of N₂O and control experiments with a Zn(II) analog verify an essential role for Cu. Theory and spectroscopy support metal-ligand cooperative catalysis between Cu(I) and a reduced tetraimidazolyl substituted radical pyridine ligand, (MeIm₄P₂Py = 2,6-(bis(bis-2-*N*-methylimidazolyl)phosphino)pyridine) which can be observed by Electron Paramagnetic Resonance (EPR) spectroscopy. Comparison with biological processes suggests a common theme of supporting electron transfer moieties in enabling Cu-mediated N₂O reduction.

Introduction

Nitrous oxide (N₂O) is the leading ozone depleting substance of this century, rivaling many hydrochlorofluorocarbons (HCFCs).¹ N₂O is also a potent greenhouse gas with a long atmospheric lifetime (> 100 years) and is 10 and 300 times more warming by mass than CH₄ and CO₂ respectively.²⁻³ Thus, decomposition of N₂O is important in order to mitigate its effect on climate. Of possible decomposition routes, the reduction of N₂O to N₂ and H₂O is attractive due to the formation of benign byproducts. However, deoxygenation remains difficult as even thermal decomposition is limited by a large kinetic barrier ($\Delta G^\ddagger = 59$ kcal/mol in the gas phase), despite being thermodynamically favorable ($\Delta G = -81$ kcal/mol).⁴⁻⁵ The poor σ -donating and π -accepting properties of N₂O lead to sluggish binding kinetics with transition metals which also limits their chemistry with N₂O.⁶⁻⁷ This problem is reflected by the small number of N₂O adducts that have been characterized structurally and/or spectroscopically.⁸⁻¹⁴

Approximately two-thirds of anthropogenic N₂O is derived from excess Haber-Bosch nitrogen (i.e. fertilizers) through incomplete bacterial denitrification.¹⁵⁻¹⁷ Some denitrification bacteria contain the gene for nitrous oxide reductase (N₂OR), the only known enzyme capable of reducing N₂O as its natural substrate to N₂ and H₂O through a 2e⁻/2H⁺ process.¹⁸ N₂OR is a Cu based metalloenzyme consisting of two Cu clusters: a binuclear copper site responsible for electron transfer, Cu_A, and a tetranuclear μ_4 -sulfido bridged cluster, Cu_Z* which is the active site for N₂O binding and reduction.¹⁹⁻²⁰ Computational and spectroscopic studies suggest that N₂OR overcomes the high kinetic barrier for N–O cleavage by binding N₂O in μ -1,3 fashion assisted by H-bonding from the secondary coordination sphere (Figure 1a),²¹⁻²² although there is some controversy over this mechanistic proposal.²³⁻²⁴ 25

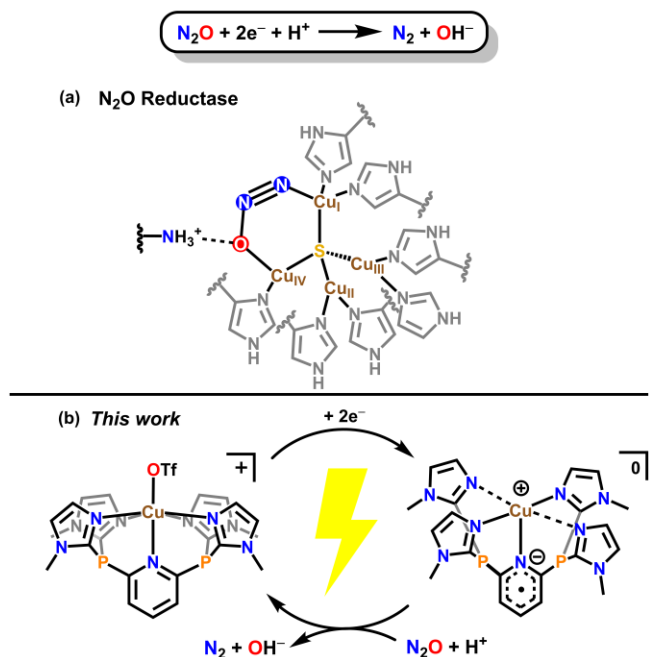


Figure 1. (a) Proposed binding of N₂O in the 4Cu₁:S active site of N₂O reductase and (b) electrochemical N₂O reduction catalysis in this work.

Despite the importance of Cu in biological N₂O reduction, and elegant synthetic work aimed at isolating structurally and chemically faithful active site mimics,²⁶⁻³³ molecular Cu catalysts for the reduction of N₂O to N₂ and H₂O/OH⁻ are not known. Nevertheless, stoichiometric reactions with di- and trinuclear Cu species suggest that tetranuclear copper sites are not required for N₂O reduction.³⁴ Favorable binding of N₂O to Cu(I) suggests that even monometallic systems should also be considered.^{8, 35}

Despite the lack of synthetic Cu-based N₂O reduction catalysts, homogeneous thermal hydrogenation of N₂O to N₂ and H₂O has been reported with 2nd and 3rd row transition metal

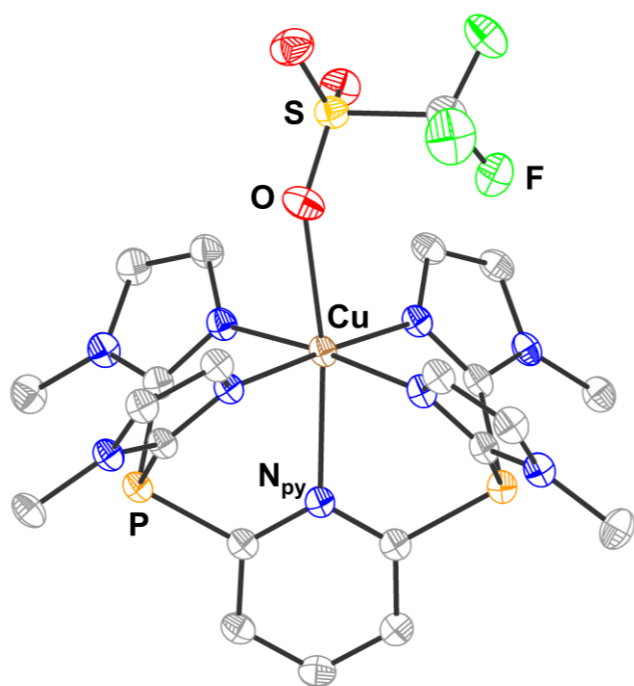


Figure 2. Solid state structure of **1-Cu**. Ellipsoids at 50% probability and hydrogen atoms have been omitted for clarity. C shown in gray, N in blue, O in red, F in green, P in orange, S in yellow, and Cu in brown. Selected bond lengths (Å) and angles (°): Cu–N_{im} 2.048(2), 2.013(2), 2.028(2), 1.997(2); Cu–N_{py} 2.432(2); Cu–O 2.487(2); O–Cu–N_{py} 170.81(7); N5–Cu–N7 87.35(8); N7–Cu–N3 92.67(8).

catalysts, namely Ru, Rh, Pt and Ir.^{36–39} Mixtures of N₂O and H₂ are potentially explosive,^{40–41} and this has also spurred interest in electrochemical reduction of N₂O as an effective route.⁴² Still, while several exciting examples of molecular N₂O electrocatalysts have recently been reported, no examples of Cu-based catalysts have been shown despite its biological relevance.^{43–48}

These considerations motivated us to investigate the synthesis of a new N₂O reduction electrocatalyst based on Cu. Herein we report the first molecular Cu complex capable of electrocatalytically reducing N₂O in MeCN using water as a proton source. Electrochemical studies show that this catalyst operates with excellent selectivity for N₂O reduction vs. hydrogen evolution. Mechanistic analysis suggests that ligand redox noninnocence plays an important role, as verified by both computations and spectroscopy, and this observation may suggest a more general need for additional electron storing ligands/metals in molecular N₂O reduction catalysis.

Results and Discussion

Catalyst Synthesis and Characterization

It has previously been shown that some organic radicals are competent outer-sphere redox catalysts for the electrochemical reduction of N₂O in MeCN,⁴⁷ and we were particularly inspired by catalysis using 4-cyanopyridine.⁴⁹ We were interested in investigating a pyridine donor that could be used as an effective electron shuttle for Cu-catalyzed N₂O

reduction (Figure 1b). Since demetallation of Cu(I) is a common deactivation pathway in Cu^{z*} synthetic models, we rationalized that polydentate chelates with strong N-donors could minimize the loss of this labile metal.^{30, 33} We previously reported a Co(II) compound supported by a tip(Me) ligand (tip(Me) = 2,6-(bis(bis-2-*N*-methylimidazolyl)-hydroxymethyl)pyridine) for electrocatalytic water oxidation which features strongly donating imidazole arms.⁵⁰ We hypothesized that strongly donating imidazole arms would chelate the metal more strongly vs. other N5 polypyridyl ligands such as PY5Me₂ (PY5Me₂ = 2,6-bis(1,1-bis(2-pyridyl)ethyl)pyridine).^{51–54} We aimed to further redesign this ligand to remove the acidic hydroxyl groups and to increase synthetic ease by replacing the carbon bridgeheads with P-atoms. This new tetraimidazolyl substituted pyridine ligand, MeIm₄P₂Py (MeIm₄P₂Py = 2,6-(bis(bis-2-*N*-methylimidazolyl)phosphino)pyridine, **1**), was synthesized by adapting a previously described one-pot reaction between a dichlorophosphine and an *N*-alkyl imidazole.⁵⁵ Addition of 2,6-(Cl₂P)Py to a mixture *N*-methylimidazole and NEt₃ in pyridine at room temperature affords **1** in good yield after workup (60 %).

Metalation was carried out by addition of Cu(OTf)₂ to a slurry of sparingly soluble **1** in MeCN, affording [(MeIm₄P₂Py)Cu(OTf)](OTf) (**1-Cu**) as an air stable blue powder in excellent yield after recrystallization (82%). Crystals suitable for single-crystal X-ray diffraction (SXRD) were obtained by slow vapor diffusion of Et₂O into MeCN at room temperature. The solid-state structure of **1-Cu** (Figure 2) reveals pentadentate coordination of **1** to Cu with one inner sphere triflate ion. This 6-coordinate species contains notably long axial bonds (Cu–O = 2.487(2) Å, Cu–N_{py} = 2.432(2) Å) consistent with a Jahn-Teller distortion in tetragonally elongated Cu(II). Imidazole bond distances (<Cu–N_{im}> = 2.022(2) Å) are slightly shorter than the non-elongated copper-pyridine distances in the analogous 6-coordinate [(PY5Me₂)Cu(MeCN)]²⁺ complex (<Cu–N_{py}> = 2.044(4) Å).⁵⁶ The metal center lies only 0.085 Å away from the plane defined by the four imidazole N-atoms. This is in contrast to our previously reported [Co(tip(Me))(CH₃CN)](OTf)₂ complex, which shows the metal “puckered” 0.213 Å away from the N_{im} plane.⁵⁰ This main structural difference between **1** and tip(Me) can be attributed to the larger size of phosphorus compared to carbon.

The frozen solution EPR spectrum of **1-Cu** (15 K) is consistent with a Cu(II), *S* = 1/2 assignment (Figure S33). Paramagnetically shifted resonances in the ¹H NMR spectrum of **1-Cu** also support this d⁹ assignment (Figure S7), and Evan’s method shows an expected solution moment of 1.71(4) μ_B. The number of resonances in the ¹H NMR is also in agreement with the solid-state C_{2v} symmetry. A sharp singlet in the ¹⁹F{¹H} NMR spectrum that is slightly shifted from free triflate suggests weakly ion paired triflate counter-anions in CD₃CN solution. Rapid ligand exchange between outer sphere triflate and MeCN is possible if not likely in solution. Additionally, a very broad resonance can be observed in the ³¹P{¹H} NMR spectrum of **1-Cu** (δ = –48 ppm) in concentrated samples, corresponding to the bridging P-atoms of the ligand with a similar chemical shift to that of **1** (δ = –45.2 ppm).

Electrochemical Characterization

Cyclic voltammetry (CV) of **1-Cu** in MeCN reveals three reduction processes. The first quasi-reversible wave at -0.8 V vs. Fc^+/Fc corresponds to a metal-centered $\text{Cu(II)}/\text{Cu(I)}$ redox couple with a large peak-to-peak separation ($\Delta E_p = 200$ mV at 100 mV s^{-1}). A similarly large ΔE_p is observed in the previously reported PY5Me_2 analog.⁵⁶ Scan rate studies show an increase in ΔE_p of **1-Cu** with increasing scan rates which indicates a changing coordination environment upon reduction from Cu(II) to Cu(I) .⁵⁷ The two remaining irreversible cathodic processes appear at $E_{p,c} = -2.15$ V and $E_{p,c} = -2.75$ V vs. Fc^+/Fc and are tentatively assigned as $\text{Cu(I)L}/\text{Cu(I)L}^{\cdot-}$ and $\text{Cu(I)L}^{\cdot-}/\text{Cu(I)L}^{2-}$ ligand-based reductions respectively ($L = \mathbf{1}$; Figure S15). These assignments are supported by the CV of **1** in MeCN which shows that the substituted pyridine ligand can be reduced by $1 e^-$ in the absence of a metal (Figure S23).

To confirm the presence of ligand-based reductions in the CV of **1-Cu**, the control complex, $[(\text{MeIm}_4\text{P}_2\text{Py})\text{ZnOTf}][\text{OTf}]$ (**1-Zn**) was synthesized following a similar procedure as its Cu(II) analog. An octahedral ligand field environment similar to that of **1-Cu** is observed in the SXR structure of **1-Zn** (Figure S36). The average Zn-N_{Im} ($2.118(1)$ Å) bond is slightly shorter than the average Zn-N_{Py} distance ($2.153(4)$ Å) in its PY5Me_2 analog, consistent with the stronger donor properties of the imidazole donors.⁵⁸ Most notably, **1-Zn** also contains an unusually long axial Zn-N_{Py} bond ($2.380(2)$ Å) which is again likely enforced by the longer bridging P-C bonds in ligand **1**.⁵⁹

The CV of **1-Zn** in MeCN shows three cathodic processes (Figure S20), with the first irreversible wave assigned as the $\text{Zn(II)L}^{2+}/\text{Zn(II)L}^{+}$ redox couple ($E_{p,c} = -1.83$ V). The remaining two, presumably ligand-based, irreversible reductions are at very negative potentials ($E_{p,c} = -2.54$ V and $E_{p,c} = -2.73$ V). Notably, the reduction of **1-Zn** is milder than that of the analogous $[\text{Zn}(\text{PY5Me}_2)(\text{MeCN})]^{2+}$ complex, suggesting that the phosphine groups in **1** are more electron withdrawing towards the apical pyridine ring.⁶⁰ The ligand-based reduction potential in **1-Zn** is significantly shifted from that of **1-Cu** ($E_{p,c} = -2.15$ V) and the free ligand **1** ($E_{1/2} = -2.68$ V). These differences in potential can be attributed to the differences in charge between the three species. Regardless of these differences, all of these CV studies support the viability of a ligand-based reduction in this system.

Electrocatalysis

In dry solvent and electrolyte, the first two reduction potentials in the CV of **1-Cu** under an atmosphere of N_2O do not shift, suggesting that there is no binding of N_2O prior to reduction of the complex (Figure 3A). Catalytic current is observed upon addition of water and a slight anodic shift is observed with increasing equivalents (Figure 3B). Reduction of N_2O occurs after the ligand is reduced as can be seen by the inflection in the catalytic wave after the $\text{Cu(I)L}/\text{Cu(I)L}^{\cdot-}$ redox couple (Figure 3A, blue trace). The slight anodic shift in the inflection point with increasing water concentration could suggest that water facilitates binding to Cu(I) and promotes N-O bond cleavage. Evidence of significant water coordination to Cu was not found as the reduction potentials of **1-Cu** remained unchanged with high

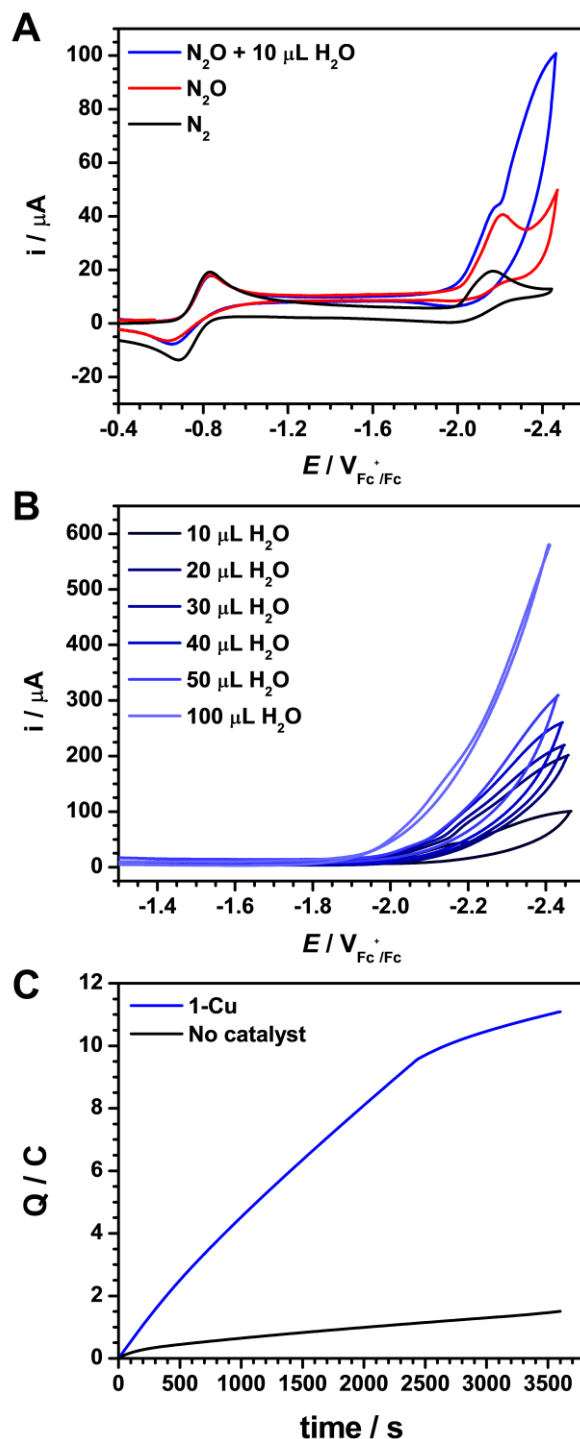


Figure 3. Cyclic voltammograms (scan rate 100 mV s^{-1}) using a 3 mm diameter glassy carbon working electrode in MeCN + 0.1 M $\text{N}^n\text{Bu}_4\text{PF}_6$ supporting electrolyte of **1-Cu** (a) under 1 atm of N_2 (black), N_2O (red) and N_2O in the presence of $10 \mu\text{L}$ (0.1 M) of water (blue); (b) **1-Cu** under 1 atm of N_2O with increasing amounts of water: $10 \mu\text{L}$ (0.11 M), $20 \mu\text{L}$ (0.22 M), $30 \mu\text{L}$ (0.33 M), $40 \mu\text{L}$ (0.44 M), $50 \mu\text{L}$ (0.55 M), $100 \mu\text{L}$ (1.11 M); (c) Controlled potential electrolysis at -2.3 V (vs Ag^+/Ag) of a MeCN solution of 0.1 M $\text{N}^n\text{Bu}_4\text{PF}_6$ supporting electrolyte with H_2O (100 mM) under 1 atm of N_2O using an RVC working electrode. Charge passed as a function of time in the presence of catalyst (**1-Cu**, 1 mM) in blue and in the absence of catalyst in black.

concentrations of water in the absence of N₂O (Figure S19). Similar electrochemical behavior is observed when NⁿBu₄OTf supporting electrolyte is used instead of NⁿBu₄PF₆ which excludes competitive OTf⁻ binding in solution (Figure S18). The CV of **1-Zn** in the presence of N₂O shows that it is not a competent N₂O reduction electrocatalyst and we note that the reduction potential of ligand **1** is beyond the onset for direct reduction of N₂O with glassy carbon (see SI for details). Both observations highlight the importance of Cu for electrocatalysis with this framework.

Controlled potential electrolysis (CPE) in the presence of 1 atm N₂O and 100 mM H₂O using a reticulated vitreous carbon (RVC) working electrode was performed at -2.3 V for 1 h to investigate the product selectivity of **1-Cu**. A linear increase of charge passed over time is seen up until ~9 C is passed after which charge consumption plateaus, indicating loss of activity (Figure 3C). This hypothesis is also supported by the slow drop in current over the course of electrolysis which suggests catalyst degradation as has been observed in related systems.⁴⁷ We note only a low amount of background activity by the RVC electrode was observed in the absence of **1-Cu** under identical conditions. Headspace analysis using TCD GC found N₂ to be the only gaseous product with no detectable H₂. An average turnover number (TON) of 54(2) was determined over the course of 1 h with a Faradaic efficiency of 83(8)% for N₂. This non-quantitative Faradaic yield likely arises from decreasing activity over time due to catalyst degradation, presumably from competing reactions with water or the OH⁻ product⁶¹ as well as limited stability of the reduced species. Further evidence of this is supported by the CV of **1-Cu** which shows the instability of the reduced species in the presence of water at slower scan rates (Figure S19). Finally, CV of the solution after CPE using a glassy carbon plate (Figure S26) shows no electrochemical features, suggesting that the decomposition product(s) are electrochemically inactive.

Mechanistic Investigations

The electrochemical activity of **1-Cu** prompted us to perform chemical and theoretical investigations of possible mechanistic steps. We hypothesized that any N₂O reduction would necessarily proceed from an initially reduced congener of **1-Cu**. We therefore investigated the reactivity of **1-Cu** with reducing agents. We initially tested catalytic chemical reduction of N₂O using 0.1% Na/Hg as a reducing agent under similar conditions to those conducted in CPE experiments (see SI). Although there is significant activity from Na/Hg and H₂O in the absence of catalyst, the presence of 1 mol % **1-Cu** more than doubles the amount of N₂ generated with nearly all reducing agent consumed (Figure S30) supporting Cu-mediated catalysis. This observation also supports using Na/Hg as a surrogate for electrochemical reduction in mechanistic probes of **1-Cu**.

We then attempted to obtain a more detailed characterization of the reduction products by chemically reducing **1-Cu** with Na/Hg in MeCN. *In situ* monitoring of this reduction by UV-visible spectroscopy shows the disappearance of the initial d-d transitions in the spectrum followed by a slow growth of two bands at approximately 410 and 680 nm over the course of 1 h (Figure S32). We propose that these absorption bands are related to the catalytically relevant

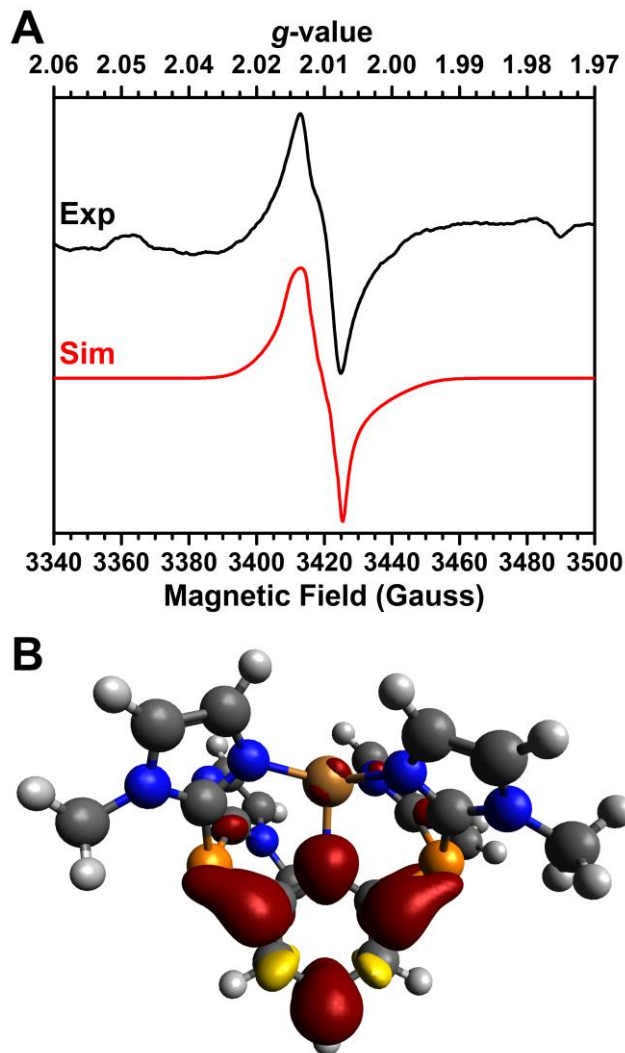


Figure 4. (A) EPR spectrum of the Na/Hg reduction of **1-Cu** and (B) Spin density plot of the 2e⁻ reduced model complex (isovalue 0.002). EPR conditions: microwave frequency 9.6304 GHz, microwave power 0.2 mW, modulation 0.03 mT/100 kHz.

species since the Cu(I) intermediate is expected to have no signal in the visible region, consistent with our observations. To test this hypothesis, characterization of this putative odd-electron reduced species was attempted using EPR spectroscopy. An EPR signal consistent with an *S* = 1/2 complex was observed in MeCN frozen solution (33 K) that is distinct from the EPR signal of the Cu(II) starting complex (Figure 4A). The frozen solution EPR spectrum of the reduction of **1-Zn** (Figure S34) shows a similar but distinct signal which supports the viability of ligand-based radicals in this system. The signal from the reduction of **1-Cu** can be simulated with *g* = 2.010, 2.013, 2.012, *A*(⁶³Cu) = 12, 11, 7 and *A*(¹⁴N) = 42, 3, 2 MHz, consistent with a primarily pyridine centered radical. We note this signal is qualitatively similar to a previously reported 2,6-disubstituted pyridine radical (broad single line, peak-to-peak 120 Gauss).⁶²

We also performed DFT calculations on possible reduced complexes to gain insight on the catalytically relevant species (Figure S38). Geometry optimizations of a singly reduced Cu(I) intermediate predict a four-coordinate geometry with one ligand arm dissociated. This prediction is consistent with the structural changes inferred from the quasi-

reversible redox couple in the CV of **1-Cu** at -0.8 V vs. Fc^+/Fc . Further reduction by an additional electron is ligand based as illustrated by the spin density which is primarily on the pyridine donor with some delocalization onto the imidazole arms through the σ^* of the P–C bond (Figure 4B). We have performed calculations of the EPR parameters of this complex which match the values obtained from simulation of the experimental spectrum well. Namely, both DFT and simulation support moderate hyperfine coupling to N and Cu (Table S1).

It is important to note that there are multiple thermodynamically accessible isomers for these reduced species which may contribute to catalyst degradation as has been reported in a similar N5 species for water reduction (see supporting information).⁶³ Thus, the depicted geometry of this doubly reduced intermediate is only a model, and other coordination geometries and ligation environments (different solvates for example) are possible if not likely. We hypothesize that this reduced species then rapidly reacts with N_2O and water to generate N_2 and OH^- , consistent with the catalytic onset which is observed just beyond the 2nd reduction event in the CV of **1-Cu**. Regardless of the exact reduced speciation of **1-Cu**, the spectroscopy and calculations support a vital role for ligand redox noninnocence as an electron storing/shuttling mechanism for catalysis. This echoes possible roles for the multi-Cu cluster in biological N_2O reduction and may point to a more fundamental requirement for additional redox cofactors in N_2O reduction catalysis by Cu.

Conclusion

We report the first example of a molecular Cu catalyst for N_2O reduction. This complex, **1-Cu**, enables electrocatalytic reduction of N_2O with water to afford N_2 with high Faradaic efficiency. Catalytic reduction with a chemical reducing agent was also demonstrated with dilute Na/Hg. Electrochemical studies support the onset of catalysis after reducing **1-Cu** twice, and a combination of spectroscopy and theory supports the importance of ligand-based reductions in forming reduced intermediates. The findings reported here provide initial proof-of-concept validation for further efforts into the design of new Cu-based molecular electrocatalysts for N_2O reduction. In addition to improved performance metrics and increasing the stability of the active catalyst, there remain interesting mechanistic questions surrounding both electron transfer principles, as well as details about N_2O binding, reduction, and protonation events.

ASSOCIATED CONTENT

Accession Codes

CCDC 2266810 and 2266811 contain the supplementary crystallographic data for this paper. These data can be obtained free of charge via www.ccdc.cam.ac.uk/data_request/cif, or by emailing data_request@ccdc.cam.ac.uk, or by contacting The Cambridge Crystallographic Data Centre, 12 Union Road, Cambridge CB2 1EZ, UK; fax: +44 1223 336033.

AUTHOR INFORMATION

Corresponding Author

* John S. Anderson - Department of Chemistry, The University of Chicago, Chicago, Illinois 60637, United States.

Authors

Jorge L. Martinez - Department of Chemistry, The University of Chicago, Chicago, Illinois 60637, United States.

Joseph E. Schneider - Department of Chemistry, The University of Chicago, Chicago, Illinois 60637, United States.

Sophie W. Anferov - Department of Chemistry, The University of Chicago, Chicago, Illinois 60637, United States.

Author Contributions

J.L.M. designed and performed experimental work and wrote the manuscript. J.E.S collected EPR data, performed computational investigations and assisted with the manuscript. S.W.A collected and refined X-ray data for the solid-state structures investigations and assisted with the manuscript. J.S.A supervised the project and assisted in writing and editing the manuscript.

Notes

The authors declare no competing financial interest.

ACKNOWLEDGMENTS

This research was supported by the National Institutes of Health (R35 GM133470). J.E.S. thanks the Department of Defense for a National Defense Science and Engineering Graduate Fellowship (00003765) and J.S.A. thanks the Sloan Foundation for a Research Fellowship (FG-2019-11497) and the Dreyfus Foundation for a Teacher-Scholar award (TC-21-064). Single crystal X-ray diffraction data reported here was collected at ChemMatCARS Sector 15 which is supported by the NSF under grant number NSF/CHE-1834750. This research used resources of the APS, a U.S. DOE Office of Science User Facility operated for the DOE Office of Science by Argonne National Laboratory under Contract No. DE-AC02-06CH11357. We would like to thank Dr. Yu-Sheng Chen for assistance with SXR data acquisition at 15-ID-B,C,D. TCD GC data was collected in the University of Chicago Mass Spectrometry facility and was supported by SF instrumentation grant CHE-1048528. The authors are grateful for the support of the University of Chicago Research Computing Center for assistance with the calculations carried out in this work. J.L.M. would like to thank Krista M. Kulesa for inspiring the research topic and insightful discussions in electrochemistry. J.L.M. would also like to thank the Wuttig group for providing helpful insights to the group for CPE experimental setup.

REFERENCES

1. Ravishankara, A. R.; Daniel, J. S.; Portmann, R. W., Nitrous Oxide (N_2O): The Dominant Ozone-Depleting Substance Emitted in the 21st Century. *Science* **2009**, *326* (5949), 123-125.
2. Rodhe, H., A Comparison of the Contribution of Various Gases to the Greenhouse Effect. *Science* **1990**, *248* (4960), 1217-1219.
3. Montzka, S. A.; Dlugokencky, E. J.; Butler, J. H., Non- CO_2 greenhouse gases and climate change. *Nature* **2011**, *476* (7358), 43-50.
4. Johnston, H. S., Interpretation of the Data on the Thermal Decomposition of Nitrous Oxide. *J. Chem. Phys.* **1951**, *19* (6), 663-667.

5. Lee, D.-H.; Mondal, B.; Karlin, K. D., Nitrogen Monoxide and Nitrous Oxide Binding and Reduction. In *Activation of Small Molecules*, 2006; pp 43-79.
6. Tolman, W. B., Binding and Activation of N₂O at Transition-Metal Centers: Recent Mechanistic Insights. *Angew. Chem. Int. Ed.* **2010**, *49* (6), 1018-1024.
7. Severin, K., Synthetic chemistry with nitrous oxide. *Chem. Soc. Rev.* **2015**, *44* (17), 6375-6386.
8. Zhuravlev, V.; Malinowski, P. J., A Stable Crystalline Copper(I)-N₂O Complex Stabilized as the Salt of a Weakly Coordinating Anion. *Angew. Chem. Int. Ed.* **2018**, *57* (36), 11697-11700.
9. Paulat, F.; Kuschel, T.; Näther, C.; Praneeth, V. K. K.; Sander, O.; Lehnert, N., Spectroscopic Properties and Electronic Structure of Pentammineruthenium(II) Dinitrogen Oxide and Corresponding Nitrosyl Complexes: Binding Mode of N₂O and Reactivity. *Inorg. Chem.* **2004**, *43* (22), 6979-6994.
10. Armor, J. N.; Taube, H., Formation and reactions of [(NH₃)₅RuN₂O²⁺]. *J. Am. Chem. Soc.* **1969**, *91* (24), 6874-6876.
11. Piro, N. A.; Lichterman, M. F.; Harman, W. H.; Chang, C. J., A Structurally Characterized Nitrous Oxide Complex of Vanadium. *J. Am. Chem. Soc.* **2011**, *133* (7), 2108-2111.
12. Gyton, M. R.; Leforestier, B.; Chaplin, A. B., Rhodium(I) Pincer Complexes of Nitrous Oxide. *Angew. Chem. Int. Ed.* **2019**, *58* (43), 15295-15298.
13. Mokhtarzadeh, C. C.; Chan, C.; Moore, C. E.; Rheingold, A. L.; Figueroa, J. S., Side-On Coordination of Nitrous Oxide to a Mononuclear Cobalt Center. *J. Am. Chem. Soc.* **2019**, *141* (38), 15003-15007.
14. Puerta Lombardi, B. M.; Gendy, C.; Gelfand, B. S.; Bernard, G. M.; Wasylishen, R. E.; Tuononen, H. M.; Roesler, R., Side-on Coordination in Isostructural Nitrous Oxide and Carbon Dioxide Complexes of Nickel. *Angew. Chem. Int. Ed.* **2021**, *60* (13), 7077-7081.
15. Richardson, D.; Felgate, H.; Watmough, N.; Thomson, A.; Baggs, E., Mitigating release of the potent greenhouse gas N₂O from the nitrogen cycle – could enzymic regulation hold the key? *Trends Biotechnol.* **2009**, *27* (7), 388-397.
16. Tavares, P.; Pereira, A. S.; Moura, J. J. G.; Moura, I., Metalloenzymes of the denitrification pathway. *J. Inorg. Biochem.* **2006**, *100* (12), 2087-2100.
17. Thomson, A. J.; Giannopoulos, G.; Pretty, J.; Baggs, E. M.; Richardson, D. J., Biological sources and sinks of nitrous oxide and strategies to mitigate emissions. *J. Philos. Trans. R. Soc.* **2012**, *367* (1593), 1157-1168.
18. Pauleta, S. R.; Dell'Acqua, S.; Moura, I., Nitrous oxide reductase. *Coord. Chem. Rev.* **2013**, *257* (2), 332-349.
19. Brown, K.; Tegoni, M.; Prudêncio, M.; Pereira, A. S.; Besson, S.; Moura, J. J.; Moura, I.; Cambillau, C., A novel type of catalytic copper cluster in nitrous oxide reductase. *Nat. Struct. Biol.* **2000**, *7* (3), 191-195.
20. Chen, P.; Gorelsky, S. I.; Ghosh, S.; Solomon, E. I., N₂O Reduction by the μ_4 -Sulfide-Bridged Tetranuclear Cu₂ Cluster Active Site. *Angew. Chem. Int. Ed.* **2004**, *43* (32), 4132-4140.
21. Gorelsky, S. I.; Ghosh, S.; Solomon, E. I., Mechanism of N₂O Reduction by the μ_4 -S Tetranuclear Cu₂ Cluster of Nitrous Oxide Reductase. *J. Am. Chem. Soc.* **2006**, *128* (1), 278-290.
22. Johnston, E. M.; Carreira, C.; Dell'Acqua, S.; Dey, S. G.; Pauleta, S. R.; Moura, I.; Solomon, E. I., Spectroscopic Definition of the Cu₂^o Intermediate in Turnover of Nitrous Oxide Reductase and Molecular Insight into the Catalytic Mechanism. *J. Am. Chem. Soc.* **2017**, *139* (12), 4462-4476.
23. Pomowski, A.; Zumft, W. G.; Kroneck, P. M. H.; Einsle, O., N₂O binding at a [4Cu:2S] copper-sulphur cluster in nitrous oxide reductase. *Nature* **2011**, *477* (7363), 234-237.
24. Wüst, A.; Schneider, L.; Pomowski, A.; Zumft, W. G.; Kroneck, P. M. H.; Einsle, O., Nature's way of handling a greenhouse gas: the copper-sulfur cluster of purple nitrous oxide reductase. *Biol. Chem.* **2012**, *393* (10), 1067-1077.
25. Johnston, E. M.; Dell'Acqua, S.; Ramos, S.; Pauleta, S. R.; Moura, I.; Solomon, E. I., Determination of the Active Form of the Tetranuclear Copper Sulfur Cluster in Nitrous Oxide Reductase. *J. Am. Chem. Soc.* **2014**, *136* (2), 614-617.
26. Johnson, B. J.; Lindeman, S. V.; Mankad, N. P., Assembly, Structure, and Reactivity of Cu₄S and Cu₃S Models for the Nitrous Oxide Reductase Active Site, Cu₂^{*}. *Inorg. Chem.* **2014**, *53* (19), 10611-10619.
27. Johnson, B. J.; Antholine, W. E.; Lindeman, S. V.; Mankad, N. P., A Cu₄S model for the nitrous oxide reductase active sites supported only by nitrogen ligands. *Chem. Commun.* **2015**, *51* (59), 11860-11863.
28. Johnson, B. J.; Antholine, W. E.; Lindeman, S. V.; Graham, M. J.; Mankad, N. P., A One-Hole Cu₄S Cluster with N₂O Reductase Activity: A Structural and Functional Model for Cu₂^{*}. *J. Am. Chem. Soc.* **2016**, *138* (40), 13107-13110.
29. Hartmann, N. J.; Wu, G.; Hayton, T. W., Synthesis and reactivity of a nickel(II) thioperoxide complex: demonstration of sulfide-mediated N₂O reduction. *Chem. Sci.* **2018**, *9* (31), 6580-6588.
30. Hsu, C.-W.; Rathnayaka, S. C.; Islam, S. M.; MacMillan, S. N.; Mankad, N. P., N₂O Reductase Activity of a [Cu₄S] Cluster in the 4Cu^I Redox State Modulated by Hydrogen Bond Donors and Proton Relays in the Secondary Coordination Sphere. *Angew. Chem. Int. Ed.* **2020**, *59* (2), 627-631.
31. Rathnayaka, S. C.; Hsu, C.-W.; Johnson, B. J.; Iniguez, S. J.; Mankad, N. P., Impact of Electronic and Steric Changes of Ligands on the Assembly, Stability, and Redox Activity of Cu₄(μ_4 -S) Model Compounds of the Cu₂ Active Site of Nitrous Oxide Reductase (N₂OR). *Inorg. Chem.* **2020**, *59* (9), 6496-6507.
32. Rathnayaka, S. C.; Islam, S. M.; DiMucci, I. M.; MacMillan, S. N.; Lancaster, K. M.; Mankad, N. P., Probing the electronic and mechanistic roles of the μ_4 -sulfur atom in a synthetic Cu₂ model system. *Chem. Sci.* **2020**, *11* (13), 3441-3447.
33. Rathnayaka, S. C.; Mankad, N. P., Coordination chemistry of the Cu₂ site in nitrous oxide reductase and its synthetic mimics. *Coord. Chem. Rev.* **2021**, *429*, 213718.

34. Sinhababu, S.; Lakliang, Y.; Mankad, N. P., Recent advances in cooperative activation of CO₂ and N₂O by bimetallic coordination complexes or binuclear reaction pathways. *Dalton Trans.* **2022**, 51 (16), 6129-6147.
35. Wang, G.; Jin, X.; Chen, M.; Zhou, M., Matrix isolation infrared spectroscopic and theoretical study of the copper (I) and silver (I)-nitrous oxide complexes. *Chem. Phys. Lett.* **2006**, 420 (1), 130-134.
36. Zeng, R.; Feller, M.; Ben-David, Y.; Milstein, D., Hydrogenation and Hydrosilylation of Nitrous Oxide Homogeneously Catalyzed by a Metal Complex. *J. Am. Chem. Soc.* **2017**, 139 (16), 5720-5723.
37. Jurt, P.; Abels, A. S.; Gamboa-Carballo, J. J.; Fernández, I.; Le Corre, G.; Aebli, M.; Baker, M. G.; Eiler, F.; Müller, F.; Wörle, M.; Verel, R.; Gauthier, S.; Trincado, M.; Gianetti, T. L.; Grützmacher, H., Reduction of Nitrogen Oxides by Hydrogen with Rhodium(I)-Platinum(II) Olefin Complexes as Catalysts. *Angew. Chem. Int. Ed.* **2021**, 60 (48), 25372-25380.
38. Ortega-Lepe, I.; Sánchez, P.; Santos, L. L.; Lara, P.; Rendón, N.; López-Serrano, J.; Salazar-Pereda, V.; Álvarez, E.; Paneque, M.; Suárez, A., Catalytic Nitrous Oxide Reduction with H₂ Mediated by Pincer Ir Complexes. *Inorg. Chem.* **2022**, 61 (46), 18590-18600.
39. Böskén, J.; Rodríguez-Lugo, R. E.; Nappen, S.; Trincado, M.; Grützmacher, H., Reduction of Nitrous Oxide by Light Alcohols Catalysed by a Low-Valent Ruthenium Diazadiene Complex. *Chem. Eur. J.* **2023**, 29 (20), e202203632.
40. Wang, L.-Q.; Ma, H.-H.; Shen, Z.-W., Explosion characteristics of H₂/N₂O and CH₄/N₂O diluted with N₂. *Fuel* **2020**, 260, 116355.
41. Wang, L.-Q.; Li, T.; Ma, H.-H., Explosion behaviors of hydrogen-nitrous oxide mixtures at reduced initial pressures. *Process Saf. Environ. Prot.* **2021**, 153, 11-18.
42. Niemann, V. A.; Benedek, P.; Guo, J.; Xu, Y.; Blair, S. J.; Corson, E. R.; Nielander, A. C.; Jaramillo, T. F.; Tarpeh, W. A., Co-designing Electrocatalytic Systems with Separations To Improve the Sustainability of Reactive Nitrogen Management. *ACS Catal.* **2023**, 6268-6279.
43. Collman, J. P.; Marrocco, M.; Elliott, C. M.; L'Her, M., Electrocatalysis of nitrous oxide reduction: Comparison of several porphyrins and binary "face-to-face" porphyrins. *J. Electroanal. Chem. Interfacial Electrochem.* **1981**, 124 (1), 113-131.
44. Taniguchi, I.; Shimpuku, T.; Yamashita, K.; Ohtaki, H., Electrocatalytic reduction of nitrous oxide to dinitrogen at a mercury electrode using niii complexes of macrocyclic polyamines. *J. Chem. Soc. Chem., Chem. Commun.* **1990**, (13), 915-917.
45. Zhang, J.; Tse, Y.-H.; Lever, A. B. P.; Pietro, W. J., Electrochemical reduction of nitrous oxide (N₂O) catalysed by tetraaminophthalocyanatocobalt(II) adsorbed on a graphite electrode in aqueous solution. *J. Porphyrins Phthalocyanines* **1997**, 1 (4), 323-331.
46. Meguru, T.; Masakazu, I., Cobalt Tetrphenylporphine Electrocatalyzed N₂O Reduction in DMF Solution. *Chem. Lett.* **1998**, 27 (10), 1017-1018.
47. Deeba, R.; Chardon-Noblat, S.; Costentin, C., Homogeneous molecular catalysis of the electrochemical reduction of N₂O to N₂: redox vs. chemical catalysis. *Chem. Sci.* **2021**, 12 (38), 12726-12732.
48. Deeba, R.; Molton, F.; Chardon-Noblat, S.; Costentin, C., Effective Homogeneous Catalysis of Electrochemical Reduction of Nitrous Oxide to Dinitrogen at Rhenium Carbonyl Catalysts. *ACS Catal.* **2021**, 11 (10), 6099-6103.
49. Deeba, R.; Chardon-Noblat, S.; Costentin, C., Molecular Catalysis of Electrochemical Reactions: Competition between Reduction of the Substrate and Deactivation of the Catalyst by a Cosubstrate Application to N₂O Reduction. *ChemElectroChem* **2021**, 8 (19), 3740-3744.
50. McMillion, N. D.; Wilson, A. W.; Goetz, M. K.; Chang, M.-C.; Lin, C.-C.; Feng, W.-J.; McCrory, C. C. L.; Anderson, J. S., Imidazole for Pyridine Substitution Leads to Enhanced Activity Under Milder Conditions in Cobalt Water Oxidation Electrocatalysis. *Inorg. Chem.* **2019**, 58 (2), 1391-1397.
51. Canty, A. J.; Minchin, N. J.; Skelton, B. W.; White, A. H., Interaction of palladium(II) acetate with substituted pyridines, including a cyclometallation reaction and the structure of [Pd{*meso*-[(py)PhMeC]₂C₅H₃N}(O₂CMe)][O₂CMe]·3H₂O. *J. Chem. Soc., Dalton Trans.* **1986**, (10), 2205-2210.
52. Bechlars, B.; D'Alessandro, D. M.; Jenkins, D. M.; Iavarone, A. T.; Glover, S. D.; Kubiak, C. P.; Long, J. R., High-spin ground states via electron delocalization in mixed-valence imidazolate-bridged divanadium complexes. *Nat. Chem.* **2010**, 2 (5), 362-368.
53. Klein Gebbink, R. J. M.; Jonas, R. T.; Goldsmith, C. R.; Stack, T. D. P., A Periodic Walk: A Series of First-Row Transition Metal Complexes with the Pentadentate Ligand PY5. *Inorg. Chem.* **2002**, 41 (18), 4633-4641.
54. Blackman, A. G., The coordination chemistry of acyclic pentadentate pentaamine ligands. *Polyhedron* **2019**, 161, 1-33.
55. Tolmachev, A. A.; Yurchenko, A. A.; Merculov, A. S.; Semenova, M. G.; Zarudnitskii, E. V.; Ivanov, V. V.; Pinchuk, A. M., Phosphorylation of 1-alkylimidazoles and 1-alkylbenzimidazoles with phosphorus(III) halides in the presence of bases. *Heteroat. Chem.* **1999**, 10 (7), 585-597.
56. Zadrozny, J. M.; Freedman, D. E.; Jenkins, D. M.; Harris, T. D.; Iavarone, A. T.; Mathonière, C.; Clérac, R.; Long, J. R., Slow Magnetic Relaxation and Charge-Transfer in Cyano-Bridged Coordination Clusters Incorporating [Re(CN)₇]^{3-/4-}. *Inorg. Chem.* **2010**, 49 (19), 8886-8896.
57. Villeneuve, N. M.; Schroeder, R. R.; Ochrymowycz, L. A.; Rorabacher, D. B., Cyclic Voltammetric Evaluation of Rate Constants for Conformational Transitions Accompanying Electron Transfer. Effect of Varying Structural Constraints in Copper(II/I) Complexes with DicyclohexanediyI-Substituted Macrocyclic Tetrathiaethers. *Inorg. Chem.* **1997**, 36 (20), 4475-4483.
58. Sun, Y.; Bigi, J. P.; Piro, N. A.; Tang, M. L.; Long, J. R.; Chang, C. J., Molecular Cobalt Pentapyridine

Catalysts for Generating Hydrogen from Water. *J. Am. Chem. Soc.* **2011**, *133* (24), 9212-9215.

59. Dudev, T.; Lim, C., Tetrahedral vs Octahedral Zinc Complexes with Ligands of Biological Interest: A DFT/CDM Study. *J. Am. Chem. Soc.* **2000**, *122* (45), 11146-11153.

60. Derrick, J. S.; Loipersberger, M.; Chatterjee, R.; Iovan, D. A.; Smith, P. T.; Chakarawet, K.; Yano, J.; Long, J. R.; Head-Gordon, M.; Chang, C. J., Metal–Ligand Cooperativity via Exchange Coupling Promotes Iron-Catalyzed Electrochemical CO₂ Reduction at Low Overpotentials. *J. Am. Chem. Soc.* **2020**, *142* (48), 20489-20501.

61. Deeba, R.; Chardon-Noblat, S.; Costentin, C., Importance of Ligand Exchange in the Modulation of

Molecular Catalysis: Mechanism of the Electrochemical Reduction of Nitrous Oxide with Rhenium Bipyridyl Carbonyl Complexes. *ACS Catal.* **2023**, 8262-8272.

62. Schröder, J.; Himmel, D.; Kratzert, D.; Radtke, V.; Richert, S.; Weber, S.; Böttcher, T., Isolation of a stable pyridine radical anion. *Chem. Commun.* **2019**, *55* (9), 1322-1325.

63. Ekanayake, D. M.; Kulesa, K. M.; Singh, J.; Kpogo, K. K.; Mazumder, S.; Bernhard Schlegel, H.; Verani, C. N., A pentadentate nitrogen-rich copper electrocatalyst for water reduction with pH-dependent molecular mechanisms. *Dalton Trans.* **2017**, *46* (48), 16812-16820.